GPS Solut
DOI 10.1007/s10291-014-0383-7

ORIGINAL ARTICLE

Using geodetic GPS receivers to measure vegetation water content

Wei Wan · Kristine M. Larson · Eric E. Small · Clara C. Chew · John J. Braun

Received: 31 October 2013 / Accepted: 2 May 2014

Abstract A GPS-based method is presented to measure vegetation water content. Commercially available geodetic-quality GPS receivers and antennas are used. The method is tested using GPS measurements collected over three field seasons. The GPS data are compared with in situ data for three plant types: desert grass, wheat, and alfalfa. The GPS retrievals of vegetation water content are based on the GPS signal-to-noise ratio (SNR) data. Instrumental issues that affect the SNR data are discussed, particularly satellite transmit power variations, footprint variations, and temperature effects. The amplitudes of the SNR data show a nearly linear relationship to the water content in grasses (0–0.5 kg/m^2) and wheat crops (0–0.9 kg/m^2). As predicted by theory, this simple linear relationship breaks down in vegetation with heavy water content, such as alfalfa. The field results are consistent with forward model predictions, whose effect restricts the use of this simple linear model for vegetation to water content of less than $\sim$1 kg/m^2.

W. Wan
School of Earth and Space Sciences, Peking University, Beijing, China

K. M. Larson (✉)
Department of Aerospace Engineering Sciences, University of Colorado Boulder, Boulder, CO, USA
e-mail: kristinem.larson@gmail.com

E. E. Small · C. C. Chew
Department of Geological Sciences, University of Colorado Boulder, Boulder, CO, USA

J. J. Braun
COSMIC, University Corporation for Atmospheric Research, Boulder, CO, USA

Keywords GNSS · GPS · SNR · Multipath · Reflections · Vegetation water content

Introduction

The primary use of the GPS constellation is real-time navigation. A much smaller community uses the same signals with advanced instruments and analysis tools for precise positioning applications in geoscience fields such as geodesy, geophysics, and glacier dynamics (Segall and Davis 1997). Since it was first suggested by Martin-Neira (1993), reflected GPS signals are also being used by geoscientists. Many of the early GPS reflection experiments were focused on altimetry (Garrison and Katzberg 2000; Gleason et al. 2005), ocean winds (Garrison et al. 2002), and soil moisture (Katzberg et al. 2005). Vegetation growth has also been the focus of many GPS reflection studies (Egido et al. 2012; Rodriguez-Alvarez et al. 2011, 2012). While the details associated with how these instruments were deployed and how the data were analyzed varies, all were designed to measure reflections. An alternative GPS reflection method, GPS-IR (GPS Interferometry Reflectometry), uses reflections that are measured by geodetic-quality GPS instruments. These instruments were not designed to measure reflections. However, it has been shown that they provide consistent measurements of upper surface soil moisture content, snow depth, and coastal sea level (Larson et al. 2008, 2009, 2013).

Small et al. (2010) first showed a qualitative agreement between reflections recorded by geodetic-quality GPS receivers and vegetation growth; however, they did not attempt a quantitative analysis. We have undertaken a two-phase effort to investigate vegetation effects in GPS-IR data. The first effort is model-based (Chew et al. 2014b). A

Published online: 17 May 2014

bare soil electrodynamic forward model, previously developed for soil moisture (Chew et al. 2014a), was modified by adding a one-dimensional, plane-stratified model for a variety of vegetation canopies. This approach, which simulates emission from vegetation canopies (Bindlish and Barros 2001), is distinct from an approach where individual components such as stalks and leaves are modeled (Mo et al. 1982). As will be discussed in the next section, these electrodynamic models predict that GPS-IR observations will be linearly correlated with vegetation water content up to values of $\sim$1 kg/m^2. Beyond this value, the relationship for GPS-IR and vegetation water content becomes nonlinear and can no longer be used to predict changes in vegetation in a forward sense. Limited comparisons were made between GPS data and field measurements for a single year.

In parallel, we have been conducting field experiments to develop retrieval algorithms for GPS-IR. Since both soil moisture and vegetation affect GPS-IR data, in situ measurements of vegetation state, precipitation, and soil moisture were made at the field sites. In order to validate these retrievals, 3 years of GPS experiments were conducted at multiple field sites. A variety of vegetation canopies were sampled, some natural and others crops. Here, we compare the experimental data for both in situ and GPS-IR and assess predictions made in Chew et al. (2014b). We also use this opportunity to explore various real-world issues related to the GPS instrumentation that must be resolved if GPS-IR is to be used to reliably measure vegetation water content.

GPS Interferometry Reflectometry

In the GPS-IR technique, the signal-to-noise ratio (SNR) data recorded by geodetic-quality GPS receivers are used to infer environmental characteristics (Larson et al. 2008, 2009). The interference between the direct and reflected signals produces a characteristic pattern in the SNR data that depends on the height of the GPS antenna above the reflecting surface, reflection coefficients for the reflecting surface, and for vegetation sensing, the water content of the vegetation. GPS-IR has bi-static radar geometry (Fig. 1). A GPS satellite transmits primarily right-handed circularly polarized (RHCP) signals at two frequencies (originally $\sim$1.5 and 1.2 GHz; a third frequency was recently added). For GPS-IR, these will be referred to as the direct signals. Since a geodetic-quality GPS antenna is designed to preferentially track this direct signal, the RHCP gains are many orders of magnitude larger than for left-handed circularly polarized (LHCP) signals. Most of the reflected energy is converted from RHCP to LHCP, with the degree of conversion depending on the surface dielectric constant and the satellite elevation angle. At elevation angles below 20°, the RHCP gains begin to taper so that reflections from the ground surface (negative elevation angles with respect to the antenna plane) can be suppressed. The choke-ring GPS antenna used by the geodetic community has very small LHCP gains in this region and thus does an excellent job of suppressing reflections from surfaces where there is a strong conversion from RHCP to LHCP from metal surfaces. However, it does a relatively poor job of suppressing reflections from natural surfaces such as soil and snow.

The GPS observation (RINEX) files report SNR data in units of decibels assuming a 1 Hz bandwidth, or dB-Hz. The strength of the direct SNR signal depends strongly on the following:

1. satellite transmit power
2. gain pattern of the receiving antenna
3. whether the code on the transmitted signal is public or encrypted.

Both L1 and L2 signals can be used for GPS-IR. The L1 GPS signal includes both a public and encrypted code. The geodetic GPS receiver used in this study (Trimble NetRS) only tracks the public L1 C/A signal. The L2 GPS signal was originally designed with only an encrypted code. Because the receiver we used lacks access to the encrypted code, these L2 measurements have much lower power than the equivalent L1 measurements. This makes it more difficult to use older L2 SNR signals for GPS-IR. Beginning in 2005, GPS began transmitting a new public code on L2 called L2C. Our research is based entirely on these new L2C signals, as were previous studies for soil moisture and snow depth (Larson et al. 2008; Larson and Nievinski 2013). Although the L1 SNR data reported by the Trimble NetRS are noisier than those from L2C (Larson et al. 2010), future studies will incorporate and compare results for both frequencies.

SNR observations for a typical L2C satellite observed with a geodetic-quality GPS unit are shown in Fig. 2. The observed direct signal is represented by the smooth low-order polynomial fit; it rises in strength by 10 dB-Hz as the satellite rises from 5 to 40° elevation angle. This rise is due primarily to a geodetic antenna's gain pattern. The bottom panel of Fig. 2 shows the SNR data after the observations have been converted to linear units, and the direct signal has been removed with a second-order polynomial. The residual SNR trace has a distinctive frequency that depends primarily on the height of the antenna above the reflecting surface (H_o, Fig. 1).

$$\begin{aligned} \mathrm{SNR} &= A(\theta) * \cos\left(\frac{4\pi H_o}{\lambda}\sin\theta + \phi_o\right) \\ &\cong A * \cos\left(\frac{4\pi H_o}{\lambda}\sin\theta + \phi_o\right) \end{aligned} \quad (1)$$

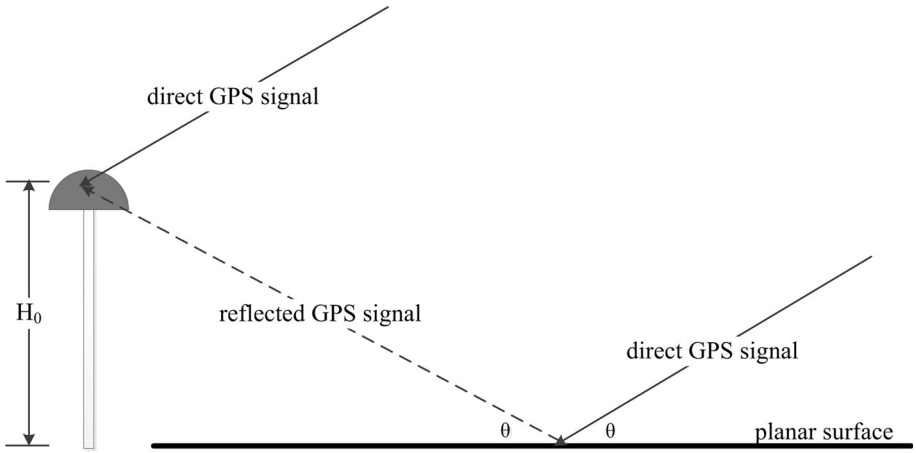

Fig. 1 Bi-static geometry of GPS-IR. θ is elevation angle of the satellite with respect to the horizon, and H_o is the apparent height of the GPS antenna phase center (depicted by the gray hemispherical dome) above the reflecting surface

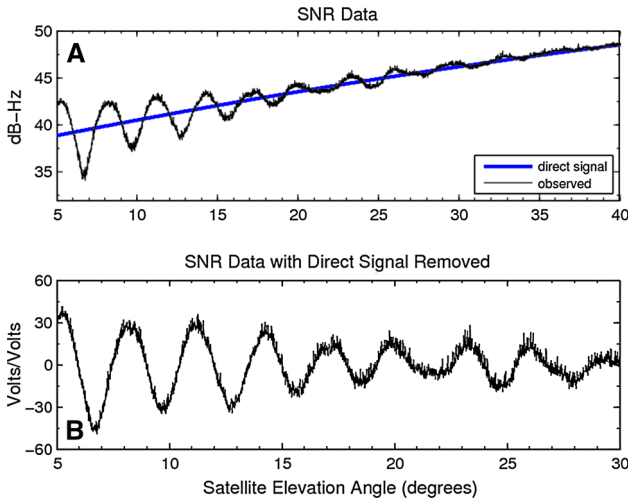

Fig. 2 **a** L2C SNR data for one GPS satellite are shown in *black*. The direct signal is represented by the smooth curve in *blue*; **b** SNR data with the direct signal removed and converted to a linear scale. Representative SNR data for the L1 C/A- and L2 P-code GPS signals can be found in Larson et al. (2010)

Equation (1) is the fixed reflector height model for GPS-IR. H_o has been referred to as the effective reflector height (Larson et al. 2010). For bare soil conditions and most soil types, H_o varies 0–5 cm as near-surface soil layers become wet and dry. For soil moisture studies, H_o is determined empirically and fixed; A and ϕ_o are then estimated using least squares. Changes in ϕ_o can then be related to soil moisture content using electrodynamic models (Chew et al. 2014a, b). For snow and sea level studies, the fixed reflector height model cannot be used. Instead, H_o is estimated using a Lomb Scargle Periodogram to determine the effective reflector height. This is then converted to snow depth or sea level height (Larson and Nievinski 2013; Larson et al. 2013). The soil moisture, snow, and sea level studies did not use the amplitude information from A.

As noted in the introduction, Chew et al. (2014b) found that the GPS-IR amplitude data were linearly related to vegetation water content up to values $\sim$1 kg/m^2, but then saturated. This linear relationship is consistent with previous radar backscatter studies (Macelloni et al. 2001). Likewise, radar studies have found the power levels saturate beyond a critical vegetation water content value (Luckman et al. 1997). Beyond vegetation water content of $\sim$1 kg/m^2, geodetic GPS instruments sense reflections from the vegetation canopy itself, not just attenuation; this means the fixed reflector height model cannot be used. Finally, this study found that GPS-IR amplitudes are also sensitive to soil moisture, introducing a 0.1–0.2 kg/m^2 error in vegetation water content estimation. These models predict that bare soil GPS-IR retrievals will have smaller amplitudes when soil is wet. The reverse is predicted when vegetation water content >0.5 kg/m^2 is present, i.e., GPS-IR amplitude retrievals increase when soil is wet.

Technical GPS issues

Before we can reliably link estimated values of A to vegetation water content, we must assess GPS-specific error sources that influence A:

1. Equation 1 is an approximation; observed SNR amplitudes still retain a small dependence on elevation angle. This means that inhomogeneities in satellite tracks such as one that begin tracking at 5° elevation angle and the other starting at 10° will result in different estimated values of A. For an ideal GPS receiver, one would be able to track all satellites in view from the same minimum elevation angle. However, many geodetic GPS systems were designed to track only 8–12 satellites at a time. As the GPS constellation is currently operating 30 % beyond its design specifications, many geodetic GPS receivers

cannot track all visible satellites. They are programmed to make decisions about the preferred signals to track. Generally, the choice is made to drop low elevation angle satellites because these signals produce noisier position estimates. This means inconsistent data sets can inadvertently be collected that show time-varying GPS amplitude signals that have no relation to vegetation water content. Because this study only uses L2C signals, we deliberately turned off tracking of 1–2 healthy GPS satellites so that no L2C data were lost. The choice of which satellite(s) to remove must be made independently for each site because satellite geometry is latitude-/longitude-dependent.

2. The GPS system consists of more than 30 satellites, with new satellites being launched on a nearly yearly basis. In the last few years, the US Department of Defense has opted to use power transmission levels that are ~4 dB-Hz higher for these newer satellites (Fig. 3). If uncorrected, these new power levels will result in larger SNR amplitude values for these satellites, which would bias estimates of vegetation water content. While not a pervasive effect, we have also identified a four-day period when the Department of Defense tested out the flexible power transmission capabilities of the new L2C satellites. This meant that power on those days was higher. If these data were not removed, the GPS amplitude data would have been interpreted as having lower vegetation water content.
3. Multiple components of a GPS instrument show a strong sensitivity to temperature, particularly the antenna preamplifier, cables, and the receiver. The latter is generally stored in a plastic box near the antenna, where it is shielded by some, but not all, of the external temperature extremes. Figure 4 shows SNR observations for an extreme case. In the winter example, the air temperature for this satellite track was −15 °C, while in summer it was 32 °C. There is a clear bias between the winter and summer data of ~1.5 dB-Hz. An analysis of a full year of SNR data shows that SNR data are strongly correlated with air temperature (Larson 2013). However, the exact relationship between the SNR data and air temperature is difficult to predict because

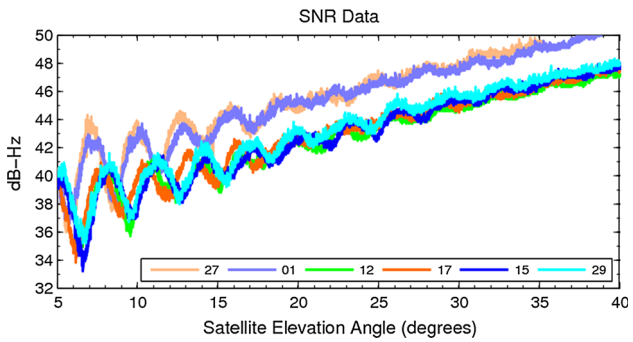

Fig. 3 Observed L2C SNR data for six GPS satellites

1. each site has different cable lengths
2. some cables are buried and some are not, and
3. the receivers are shielded from temperature extremes in different ways.

Even though the temperature bias appears to be large, once the direct signal component is removed with a polynomial, the discrepancy between summer and winter data is much less apparent. Figure 4 also shows SNR data corrected for temperature using a linear relationship between air temperature and SNR. While the raw SNR data agree much better with each other than the original summer and winter observations, the improvement for the SNR data after the direct signal removed is very small.

Finally, the issue of the GPS reflection footprint needs to be addressed. The GPS-IR footprint for a single rising or setting satellite depends on H_o and the GPS signal wavelength; for L2C, the wavelength is ~24.4 cm. It is an elongated ellipse in the direction of the satellite track (Larson and Nievinski 2013). As the satellite rises and elevation angle increases, the Fresnel zone gets smaller and closer to the GPS antenna. Figure 5 summarizes the general features of the Fresnel zones for GPS satellites available for the time period of 2010–2012. For sites at mid-northern latitudes, there are no satellite tracks between azimuths of ~320 and 40°. For sites in natural environments, all of the satellite tracks in Fig. 5 could be used. Only the southern tracks will be used in this study because the farmers requested that we deploy the GPS instruments at the northern ends of their agricultural fields. We considered using some of the more easterly and westerly satellite tracks, but opted not to because the fields on either side of our agricultural experiments were either fallow or growing a different crop.

Figure 5 also makes clear that the GPS-IR reflection footprint is far from homogeneous. For an antenna that is 2 m high and a satellite at elevation angle of 5°, it extends a radial distance of over 60 m; however, this spatial sampling quickly reduces to ~20 m at an elevation angle of 10°. Standard retrievals using GPS-IR have used elevation angle ranges of 5–30° to ensure that the frequency of the SNR data can be reliably retrieved (Larson et al. 2010; Larson and Nievinski 2013). This means that a large percentage of the data are collected within 10 m of the antenna. The sampling footprint can easily be increased in size by raising the height of the GPS antenna, but this does not make the footprint homogeneous.

Previous GPS-IR analyses have assumed that the Fresnel zones for a reflection experiment do not vary. Figure 6 shows that this is a good assumption. Except for one

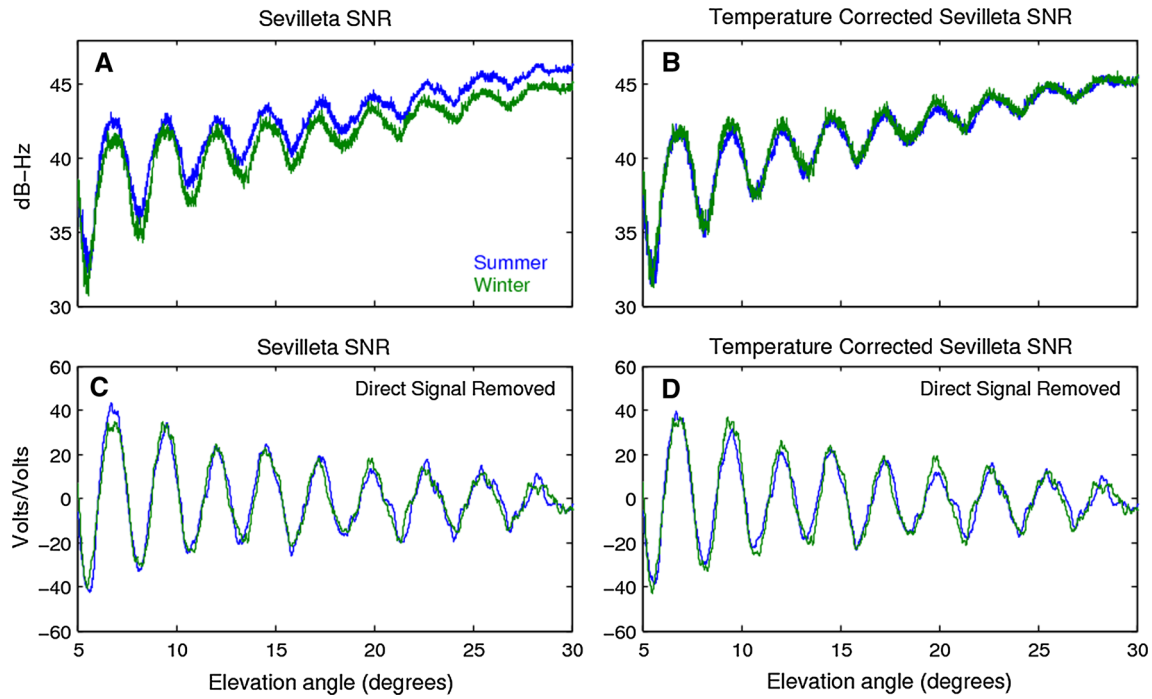

Fig. 4 Representative SNR data showing the impact of temperature corrections. **a** L2C SNR data in dB-Hz for the Sevilleta grasslands site for representative winter and summer days; **b** L2C SNR data corrected assuming a linear relationship between SNR data and temperature; **c** SNR data converted to a linear scale with direct signal removed; **d** temperature-corrected SNR data converted to a linear scale with direct signal removed. A 15-point smoother has been run on the linear scale data

satellite, the GPS-IR footprint varies by only 3–5 m. In 2010, satellite 15 shows a spread of $\sim$10 m in its footprint. This is indicative of orbit maneuvering by the US Department of Defense. This was the only significant change between 2010 and 2012 for the 7 satellites used in this study.

The analysis of the GPS SNR data in this paper can be summarized as follows:

1. For each day, the direct signal of the SNR data for the satellite tracks (Fig. 2) was removed with a second-order polynomial. The residual, using a linear scale, was fit to Eq. (1), i.e., the fixed reflector height model. Least squares was used to estimate A and ϕ_o. The effective reflector height that defines H_o for each satellite track was estimated using $\sim$30 days of bare soil conditions and fixed throughout.
2. To remove effects of variable transmit power, the estimated amplitudes for each satellite track were normalized relative to their bare soil values ($A_{norm} = A/A_{baresoil}$). Thus, normalized amplitude values of 1 are for bare soil.
3. A daily amplitude value was then constructed using the mean of the individual normalized satellite amplitudes.
4. For agricultural sites, the data before and after the fields were plowed were discarded because this changes surface roughness and effective reflector height. For all sites, data impacted by snow were removed.

GPS data

We used data from five sites in this study. Two GPS receivers were deployed at the Sevilleta Long-Term Ecological Research Station (http://sev.lternet.edu). These sites are approximately 100 km south of Albuquerque, New Mexico. One GPS receiver measured desert grassland, and the other receiver was installed on shrubland. The remaining field sites were located near to Boulder, Colorado, which is $\sim$50 km northwest of Denver. The first site, Marshall Field, has vegetation characterized as short-grass steppe. The other GPS receivers were deployed in agricultural fields. One of these sites was planted with alfalfa in each of the years from 2010 to 2012. The crop was harvested 3–4 times each summer. The other site was located near a wheat field in 2010 and 2011 and an oat crop in 2012. For simplicity, we will always call this the wheat site. Only one crop is harvested each year at the wheat site; it is not irrigated. All of the sites had identical GPS equipment: a Trimble netRS geodetic-quality dual-frequency receiver. The choke-ring antenna was covered by a radome. The receivers all

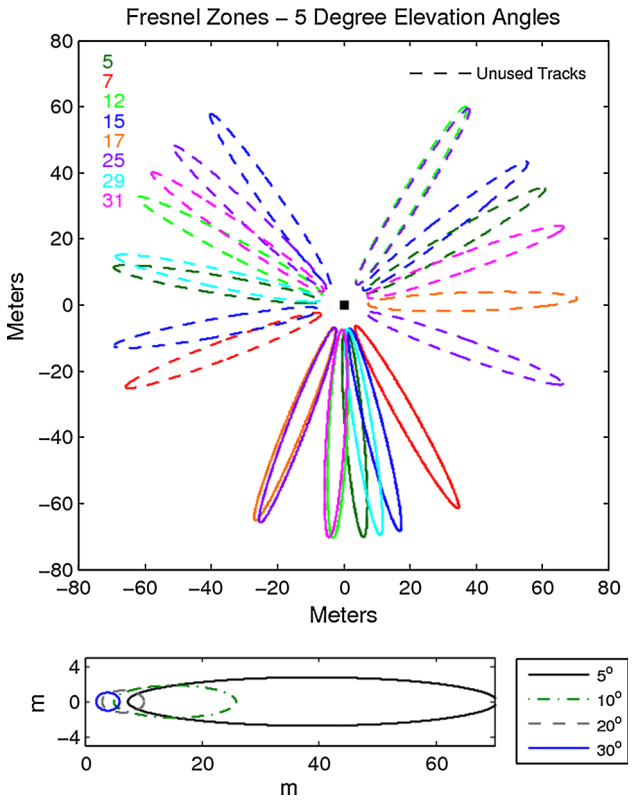

Fig. 5 The footprint of the GPS method is approximated by the first Fresnel zone. This depends on the satellite azimuth and height of the antenna above the reflecting surface. *Top* first Fresnel zones computed for an elevation angle of 5° for a GPS antenna that is 2 m tall and situated at Marshall, Colorado. The satellite numbers used in this study are shown on the left. The GPS antenna is located at the coordinates 0.0. *Dashed lines* indicate Fresnel zones for satellites tracks that are not used; *Bottom* Fresnel zones for elevation angles of 5, 10, 20, and 30°. The GPS antenna is again located at the coordinates 0.0

operated at 1 sample per second and tracked the new L2C signal as well as the legacy L1 and L2 signals. The antennas were 2–2.4 m above the ground. As will be discussed later, there were drought conditions in Boulder in 2012. This significantly affected all the data collected in Boulder that year.

Temperature, precipitation, and soil moisture data

Temperature and precipitation were measured every 5 min with a Vaisala WXT520 sensor collocated with the GPS receiver. Soil moisture was measured every 30 min at depths of 2.5, 7.5, and 20 cm using Campbell Scientific 616 soil moisture probes. Typically, five sensors were placed at 2.5 and 7.5 cm, and two sensors were placed at 20 cm. The soil moisture sensors were placed within the GPS footprint.

In situ vegetation data

During the growing season at the Boulder sites, in situ vegetation data were measured on a nearly weekly basis (Fig. 7). A 30 cm by 30 cm quadrat was thrown randomly in 7 different locations within 7–35 m from the GPS antenna. The distances and azimuths were recorded. For each vegetation sample, the plants within the quadrant were clipped and weighed immediately. This will be called the wet weight. The samples were bagged, dried in an oven for 48 h at 50 °C, and then weighed again; this is the dry weight. Vegetation water content is the difference between the wet weight and dry weight. It should be noted that the sampling procedure changed between 2010 and the following years. In 2010, we sampled between 7 and 75 m from the GPS antenna, whereas in subsequent years, we only sampled between 7 and 35 m (as stated above). This was due to the fact that at the end of 2010, we refined our Fresnel zone estimates and concluded that most of the reflected signal was actually coming from closer to the antenna. We also collected in situ vegetation data more frequently in 2011 and 2012 than we did in the first field season.

Although we compute statistics for these in situ vegetation measurements, we cannot expect the means or standard deviations to completely characterize the state of vegetation on any given day. The natural environment surrounding most GPS antennas includes widely varying vegetation cover, even within one field site. The inhomogeneous vegetation that exists is not guaranteed to follow a normal distribution, and seven samples are not enough to determine whether any such distribution exists. However, taking more samples could have significantly altered the field sites over time and thus altered our conclusions in this study. Despite this, we do see seasonal variations in our vegetation measurements and therefore use them to interpret our results in a general sense.

Vegetation height was also measured at each site. For these measurements, we recorded the 90 % canopy height. This was done so as to minimize anomalously high measurements that could have been caused by reporting the absolute maximum height. Figure 7 summarizes the in situ vegetation measurements. At Marshall, the vegetation water contents peaked at $\sim$0.5 kg/m^2 in 2010 and 2011, but show almost no growth during the drought year in 2012. Average height values are below 40 cm. At the wheat site in 2010–2011, water content values range from 0 to 0.9 kg/m^2 and peak heights were also slightly higher than at Marshall, $\sim$80 cm. However, the wheat crop in 2012 was drastically impacted by the drought, with significantly lower heights and water content. At the alfalfa field, vegetation water content measurements are almost ten times higher, reaching as values of 4.5 kg/m^2. This is because the farmers irrigate the alfalfa field, but not the wheat field. Vegetation heights peaked at $\sim$100 cm.

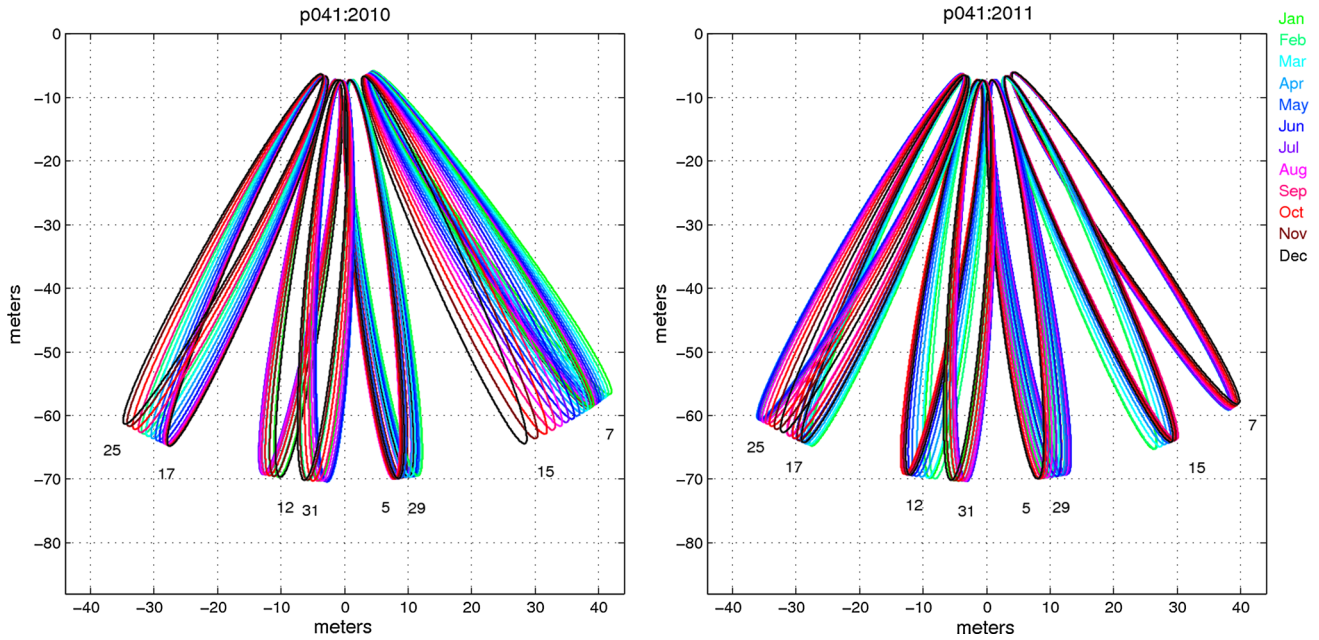

Fig. 6 First Fresnel zones computed each month for the years 2010 and 2011 at Marshall Field, Colorado. The assumed antenna height is 2 m, and the elevation angle depicted is 5°. Satellite numbers are given below the Fresnel zones

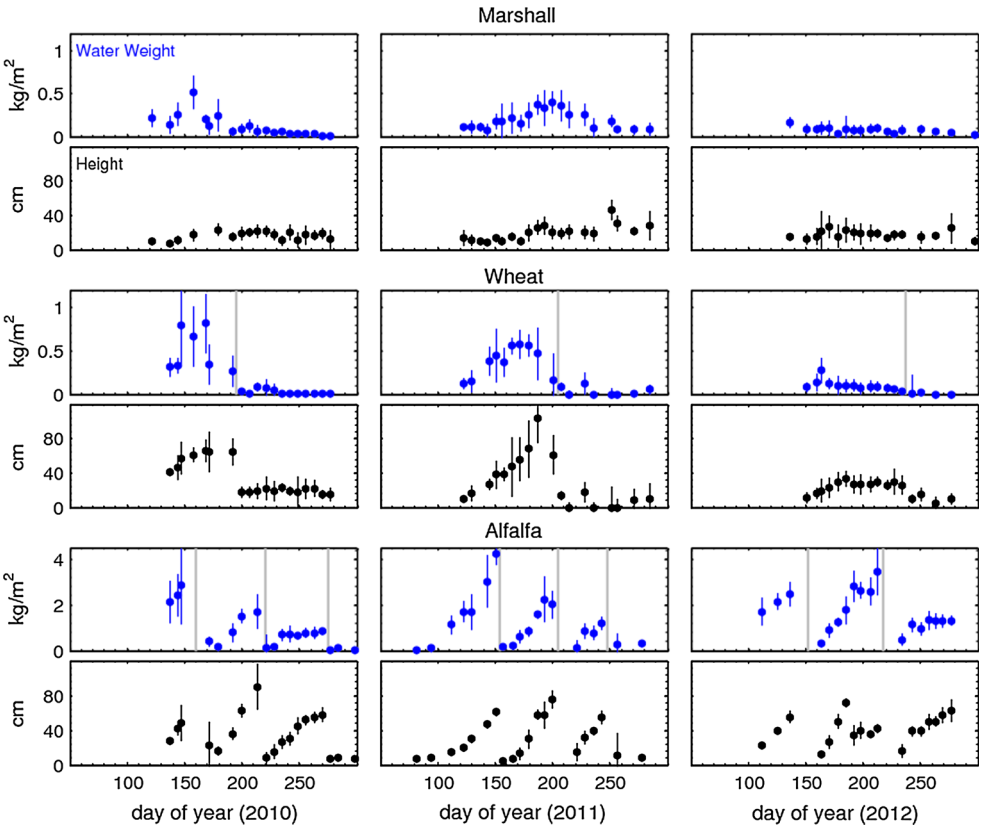

Fig. 7 *In situ* field measurements of vegetation water content and vegetation height. Each measurement is the mean, and the *error bar* represents the standard deviation of the individual measurements. *Gray lines* indicate the approximate timing of the crop harvest

Results

Following the protocol described in the previous section, time series of normalized GPS amplitude for each GPS satellite were estimated for each field site for the years 2010, 2011, and 2012. Before assessing the relationship between mean GPS amplitudes and vegetation growth, we will first use these time series to assess the internal

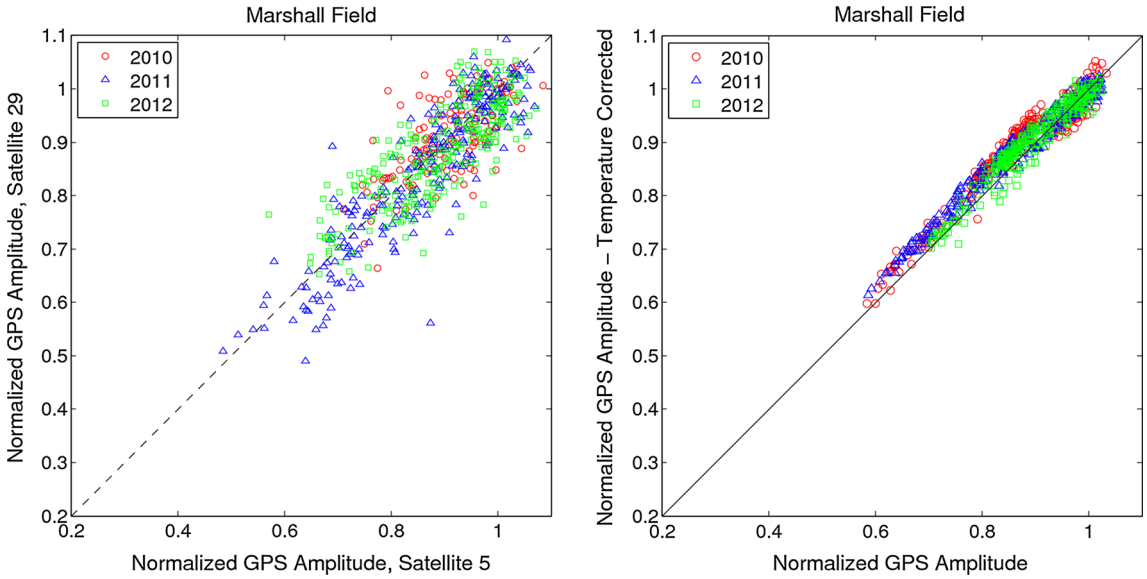

Fig. 8 Normalized GPS amplitudes are evaluated for satellite and temperature biases. *Left* comparison of normalized amplitude retrievals for satellites 5 and 29 at Marshall Field between 2010 and 2012; *Right* comparison of normalized amplitudes, with and without a temperature correction

consistency of the solutions. The average normalized GPS amplitudes will produce an unbiased estimate of amplitude if the individual satellite track retrievals are themselves unbiased. This assumption can be tested by assessing the agreement between individual satellite amplitude retrievals. Figure 8 compares the normalized amplitude retrievals over 3 years for satellites 5 and 29 at Marshall Field; these satellites have adjacent footprints. There is a small bias in the normalized amplitude units of 0.05 for all 3 years. Although the temperature dependence appeared to be small, we also compared 3 years of solutions for Marshall Field. The impact of an uncorrected temperature bias is even smaller, 0.01 in normalized amplitude units (Fig. 8).

Representative GPS amplitude time series for the four field sites (Sevilleta shrublands, Marshall, wheat, and alfalfa) are shown in Fig. 9. Sevilleta amplitudes vary little from a bare soil value of 1. This is consistent with a limited number of in situ measurements made in 2010, where vegetation water content was $\sim$0.01–0.02 kg/m^2. The largest amplitude excursions in the GPS amplitude time series coincide with soil moisture variations (not shown) that are the result of precipitation events. As predicted, soil moisture variations at a bare soil site like Sevilleta produce decreases in GPS amplitudes. To emphasize this point, timing for large precipitation events is plotted as gray vertical lines along with the GPS amplitudes. The lower panel shows the dominant effective reflector height estimated using the Lomb Scargle Periodogram relative to the *A* we used in the fixed reflector height model and estimated using least squares. At the Sevilleta site, effective reflector height varies by less than a centimeter—and only at times when the precipitation gauge indicates that it rained. This is consistent with electrodynamic forward models (Zavorotny et al. 2010; Chew et al. 2014b). At Marshall, the normalized GPS amplitudes (Fig. 9) roughly agree with the growing cycle seen in the in situ vegetation data (Fig. 7). In contrast to Sevilleta, changes in effective reflector height are more pronounced at this site, as was noted in a previous soil moisture paper on the Marshall site (Larson et al. 2010).

At the wheat site, the GPS amplitudes are consistent in timing with the measured vegetation water content data. However, those GPS amplitude changes are mirrored by changes in reflector height variations. As the wheat crop grows, the estimated reflector height gets closer to the antenna by 3–4 cm. It returns closer to its initial value after the crop is harvested. There are also large positive amplitude excursions at the wheat site at $\sim$day of year 175 and 190. These are also days with large precipitation events. Again, this is consistent with model predictions for soil moisture variations with a vegetation canopy (Chew et al. 2014b). After the wheat crop has been harvested (and the field better approximates bare soil), precipitation events are accompanied by decreases in GPS amplitudes.

Finally, we examine the GPS amplitude retrievals for alfalfa. Except for a few weeks between each of the alfalfa crops, the dominant reflector height is far from the effective reflector height used to estimate those amplitudes. In other words, the constant reflector height model used to

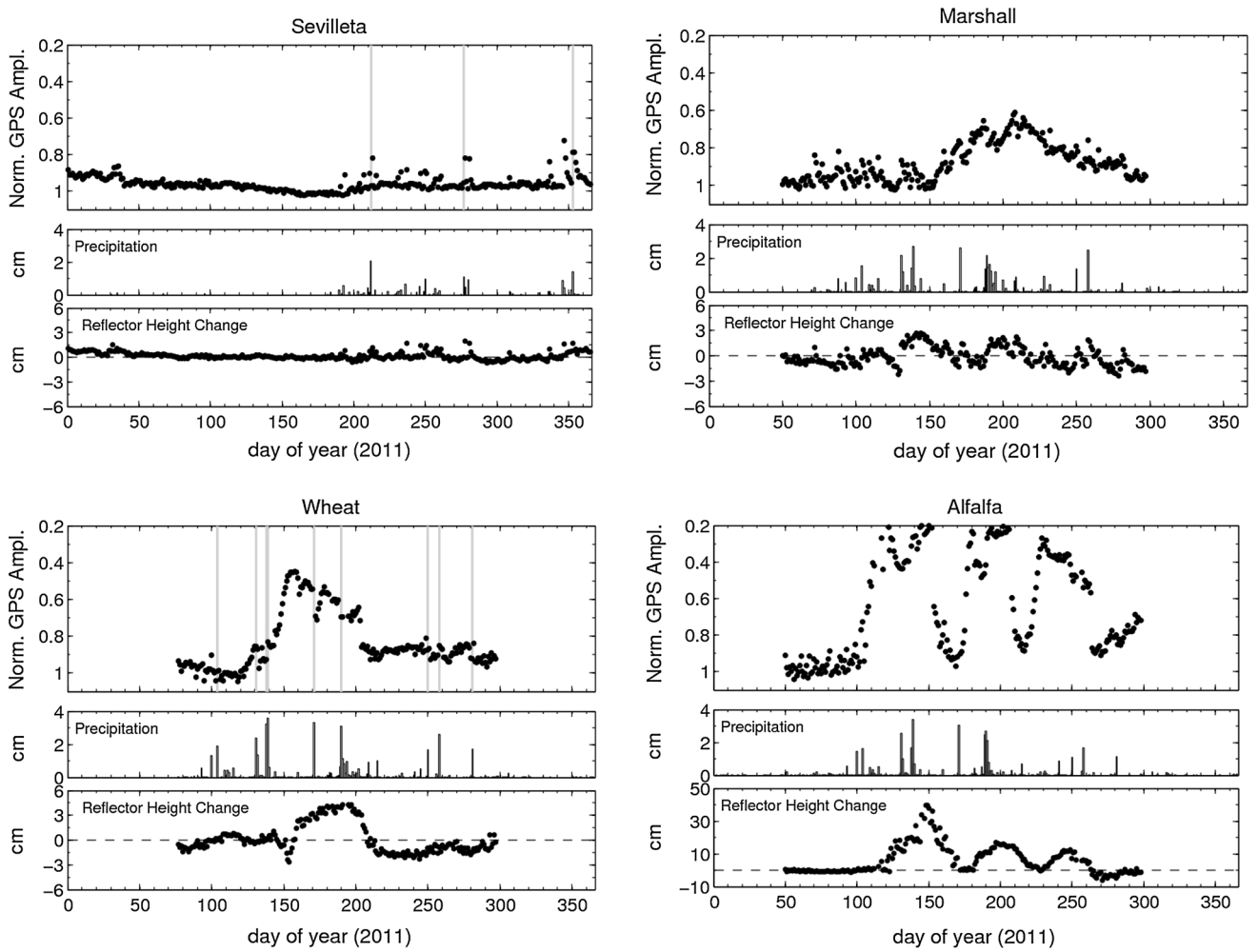

Fig. 9 Normalized GPS amplitudes are compared with precipitation and reflector height changes. *Top panels* normalized GPS amplitudes for the Sevilleta shrubland, Marshall, wheat, and alfalfa sites in 2011; middle panel: daily precipitation values; *bottom*: estimated effective reflector height. Note change in the reflector height change scale for the Alfalfa field. Large precipitation events for the Sevilleta and wheat sites are highlighted by *gray lines* in the amplitude time series

derive these amplitudes is invalid because the reflector height used in least-squares estimation of amplitude is not close to the dominant reflector height in the SNR data. We can see more detail of how the constant reflector height model breaks down in Fig. 10. Here, the estimated reflector height values are plotted as a function of the in situ vegetation water content. When the vegetation water content value is low (0–0.5 kg/m^2), GPS amplitude values are relatively close to bare soil values (0.8–1.0). However, as vegetation water content increases, the GPS amplitudes quickly drop, and the dominant effective reflector height observed in the SNR data moves closer to the antenna, i.e., in the direction of vegetation growth. Again, this result is consistent with forward models (Chew et al. 2014b)

Figures 11 and 12 summarize the amplitude–vegetation water content relationship for the Marshall and wheat fields. The uncertainties shown are based only on the standard deviation of the observations. While the measurements in 2011 are fairly consistent, the 2010 measurements show very poor agreement between the GPS results and in situ data. While the measurement protocol changed between 2010 and 2011 to emphasize the region closer to the GPS antenna, it is not clear that this is responsible for the discrepancy. The in situ measurements in 2010 were also less precise than in subsequent years. There is almost no measured vegetation water content in 2012. Using all 3 years of data, the R^2 value is 0.3. The wheat data show a much stronger correlation between the GPS and in situ data, with a R^2 0.7. Some of the misfit between GPS and the in situ data is caused by soil moisture variations. This error is predicted to be on the order of 0.1–0.2 kg/m^2. These field studies would translate to an

error of 10–20 % for vegetation water content estimates (Chew et al. 2014b).

The amplitudes of GPS SNR data are clearly sensitive to vegetation growth in general, and vegetation water content specifically. However, SNR data are also sensitive to soil moisture content, which complicates our ability to isolate vegetation water content. Furthermore, the gain pattern of a geodetic antenna is a significant restriction on using this system for vegetation monitoring. GPS-IR applications such as snow depth and sea level were primarily geometry-driven, meaning that the frequency of the SNR interference pattern was used. SNR phase retrievals have also been shown to be robust for soil moisture (Larson et al. 2010; Chew et al. 2014a, b). However, SNR amplitudes are sensitive to multiple factors. This makes it difficult to uniquely derive vegetation water content using GPS-IR. While a geodetic GPS receiver could still be used, an antenna that was designed to measure vegetation growth—analogous to the ones used by in GPS vegetation monitoring experiments (Rodriguez-Alvarez et al. 2011; Egido et al. 2012)—would yield much stronger results. One side benefit of the GPS SNR amplitudes and associated effect reflector heights shown here is that they can be used to identify times when soil moisture estimates derived using GPS-IR have been contaminated by vegetation growth. In fact, the amplitudes and reflector height variations shown are being used for quality control of soil moisture estimates derived from a large GPS network in the western USA (Larson and Small 2013).

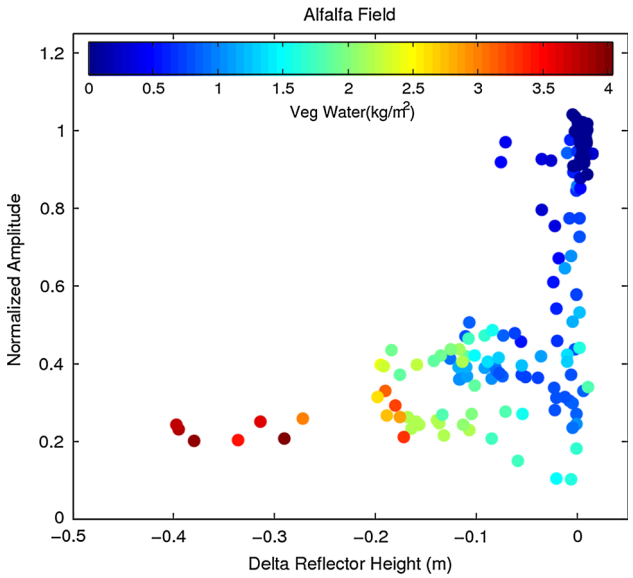

Fig. 10 Change of effective reflector height estimated for the alfalfa field in 2011 is compared with normalized GPS amplitude. *Color coding at top* shows interpolated values for measured vegetation water content

Conclusions

This study assesses the agreement between GPS reflection data and measured vegetation water content for 3 years of data from natural environments and agricultural fields. The GPS instrument used in the experiments is not designed for vegetation sensing; it is most typically used by geodesists and surveyors. A normalization method is proposed to minimize the effect of satellite track inhomogeneities. The influence of temperature on the GPS data was evaluated and found to be small compared to the typical noise in the GPS SNR data. The GPS data are sensitive to the water content in plant types such as desert grasses and agricultural crops such as wheat. However, the very simple model used to model variations in amplitude breaks down in high water content crops such as alfalfa. This is consistent with

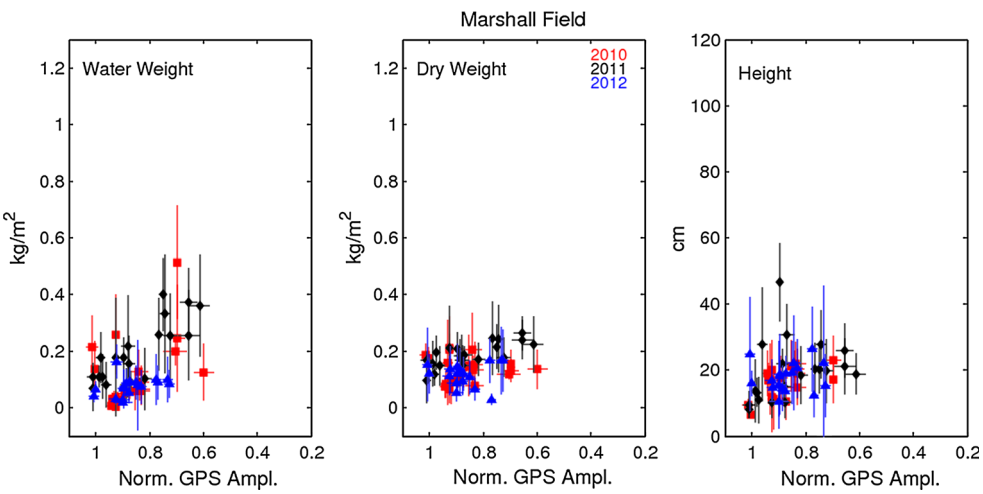

Fig. 11 GPS amplitude–vegetation relationships for the Marshall field. *From left to right* water weight, dry weight, and height. Both the GPS uncertainties and the in situ vegetation water weight uncertainties are based on the observation standard deviation (repeatability). The regression yields VWC = $-0.51A_{\mathrm{norm}} + 0.56$

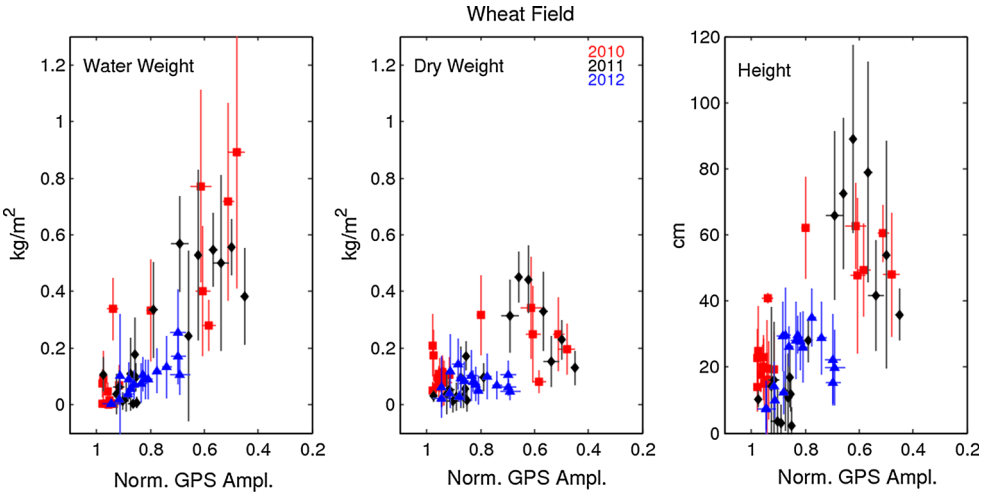

Fig. 12 GPS amplitude–vegetation relationships for the wheat field. *From left to right* water weight, dry weight, and height. Both the GPS uncertainties and the in situ vegetation water weight uncertainties are based on the observation standard deviation (repeatability). The regression yields VWC = $-1.18A_{\text{norm}} + 1.13$

model predictions (Chew et al. 2014b), restricting its use for vegetation water contents of less than ~ 1 kg/m^2.

Acknowledgments The first author's visit to the University of Colorado was funded by China Scholarship Council, File No. 201206010122. The University of Colorado was funded by NSF AGS0935725 and EAR1144221.

References

Bindlish R, Barros AP (2001) Parameterization of vegetation backscatter in radar-based, soil moisture estimation. Remote Sens Environ 76(1):130–137

Chew CC, Small EE, Larson KM, Zavorotny VU (2014a) Effects of near-surface soil moisture on GPS SNR data: development of a retrieval algorithm for soil moisture. IEEE Trans Geosci Rem Sens 52(1):537–543. doi:10.1109/TGRS.2013.2242332

Chew CC, Small EE, Larson KM, Zavorotny VU (2014b) Utility and limitations of GPS-interferometric reflectometry in vegetation sensing. IEEE Trans Geosci Rem Sens. (submitted for publication); reviewed and revised

Egido A, Caparrini M, Ruffini G, Paloscia S, Santi E, Guerriero L, Pierdicca N, Floury N (2012) Global navigation satellite systems reflectometry as a remote sensing tool for agriculture. Rem Sens 4(8):2356–2372. doi:10.3390/rs4082356

Garrison JL, Katzberg SJ (2000) The application of reflected GPS signals to ocean remote sensing. Rem Sens Environ 73(2):175–187. doi:10.1016/s0034-4257(00)00092-4

Garrison JL, Komjathy A, Zavorotny VU, Katzberg SJ (2002) Wind speed measurement using forward scattered GPS signals. IEEE Trans Geosci Remote Sens 40(1):50–65

Gleason S, Hodgart S, Yiping S, Gommenginger C, Mackin S, Adjrad M, Unwin M (2005) Detection and processing of bistatically reflected GPS signals from low Earth orbit for the purpose of ocean remote sensing. IEEE Trans Geosci Rem Sens 43(6):1229–1241. doi:10.1109/TGRS.2005.845643

Katzberg SJ, Torres O, Grant MS, Masters D (2005) Utilizing calibrated GPS reflected signals to estimate soil reflectivity and dielectric constant: results from SMEX02. Rem Sens Environ 100(1):17–28. doi:10.1016/j.rse.2005.09.015

Larson KM (2013) A methodology to eliminate snow and ice-contaminated solutions from GPS coordinate time series. J Geophys Res 118(8):4503–4510. doi:10.1002/jgrb.50307

Larson KM, Nievinski FG (2013) GPS snow sensing: results from the EarthScope plate boundary observatory. GPS Solut 17(1):41–52. doi:10.1007/s10291-012-0259-7

Larson KM, Small EE (2013) Using GPS to study the terrestrial water cycle. EOS Trans AGU 94(52):505–506

Larson KM, Small EE, Gutmann ED, Bilich AL, Braun JJ, Zavorotny V (2008) Use of GPS receivers as a soil moisture network for water cycle studies. Geophys Res Lett 35:L24405. doi:10.1029/2008GL036013

Larson KM, Gutmann ED, Zavorotny V, Braun A, Williams MW, Nievinski FG (2009) Can we measure snow depth with GPS receivers. Geophys Res Lett 36:L17502. doi:10.1029/2009GL039430

Larson KM, Braun JJ, Small EE, Zavorotny VU, Gutmann ED, Bilich AL (2010) GPS multipath and its relation to near-surface soil moisture content. IEEE JSTARS 3(1):91–99. doi:10.1109/JSTARS.2009.2033612

Larson KM, Löfgren JS, Haas R (2013) Coastal sea level measurements using a single geodetic GPS receiver. Adv Space Res 51(8):1301–1310. doi:10.1016/j.asr.2012.04.017

Luckman A, Baker J, Kuplich TM, Freitas C, Frery AC (1997) A study of the relationship between radar backscatter and regenerating tropical forest biomass for spaceborne SAR instruments. Rem Sens Environ 60:1–13

Macelloni G, Paloscia S, Pampaloni P, Marliani F, Gai M (2001) The relationship between the backscattering coefficient and the biomass of narrow and broad leaf crops. IEEE Trans Geo Rem Sens 39(4):873–884. doi:10.1109/36.917914

Martin-Neira M (1993) A Passive Reflectometry and Interferometry System (PARIS)-application to ocean altimetry. ESA J 17(4):331–355

Mo T, Choudhury BJ, Schmugge TG, Wang JR, Jackson TJ (1982) A model for microwave emission from vegetation-covered fields. J Geophys Res 87(1):11229–11237

Rodriguez-Alvarez N, Camps A, Vall-llossera M, Bosch-Lluis X, Monerris A, Ramos-Perez I, Valencia E, Marchan-Hernandez JF, Martinez-Fernandez J, Baroncini-Turricchia G, Perez GC, Sanchez N (2011) Land geophysical parameters retrieval using the interference pattern GNSS-R technique. IEEE Trans Geosci Rem Sens 49(1):71–84. doi:10.1109/TGRS.2010.2049023

Rodriguez-Alvarez N, Bosch-Lluis X, Camps A, Ramos-Perez I, Valencia E, Hyuk P, Vall-llossera M (2012) Vegetation water

content estimation using GNSS measurements. IEEE Geosci Rem Sens Lett 9(2):282–286. doi:10.1109/LGRS.2011.2166242

Segall P, Davis J (1997) GPS applications for geodynamics and earthquake studies. Ann Rev Earth Planet Sci 25:301–336. doi:10.1146/annurev.earth.25.1.301

Small EE, Larson KM, Braun JJ (2010) Sensing vegetation growth with reflected GPS signals. Geophys Res Lett 37(12):L12401. doi:10.1029/2010GL042951

Zavorotny VU, Larson KM, Braun JJ, Small EE, Gutmann ED, Bilich AL (2010) A physical model for GPS multipath caused by land reflections: toward bare soil moisture retrievals. IEEE JSTARS 3(1):100–110. doi:10.1109/JSTARS.2009.2033608